Hindawi
Advances in Materials Science and Engineering
Volume 2020, Article ID 1020732, 13 pages
https://doi.org/10.1155/2020/1020732

Research Article

Study on Internal Force of Tunnel Segment by Considering the Influence of Joints

Linwei Dong, Zhiyong Yang, Zhenyong Wang, Yaowen Ding, and Weiqiang Qi

School of Mechanics and Civil Engineering, China University of Mining and Technology-Beijing, Beijing 100083, China

Correspondence should be addressed to Zhiyong Yang; yangzy1010@126.com

Received 14 August 2020; Revised 11 October 2020; Accepted 15 October 2020; Published 31 October 2020

Academic Editor: Shengwen Tang

The mechanical performance of segments is an important aspect of the safety of tunnel structures. Study on the internal force of tunnel segment by considering the influence of joints is beneficial for obtaining a better understanding of the influence of various factors on the internal force of the segments. Based on the mechanical characteristics of shield segment joints, in which the displacements and stiffness are discontinuous, a mechanical model of the segment component under the constraints of elastic support was established. The elastic centre method and the principle of superposition were used to quantify the influence of joint displacements on the internal force of the segment component. Combined with a practical engineering application, the internal force of the segment component with joint rotation and dislocation was analysed. The displacements of the segment joints cause an unloading effect of the corresponding internal force of the joints, leading to internal force redistribution of each segment cross section. According to the spline interpolation results of the load test data of the segment joints, the internal force of the segment component under an external load is solved by the iterative method.

1. Introduction

The influences of the joints on the internal forces should be taken into consideration in the design of the segment structure [1–3]. According to joint simplification, some methods have been proposed to calculate the segment, including mainly the uniform rigid ring [4–6], multihinge ring [7, 8], and beam-spring model [3, 9–11], as shown in Figure 1. Among the above three models, the beam-spring model is the most widely used one in the calculation of the segment ring. In the beam-spring model, since the joint stiffness has a significant influence on the internal force of the segment [12–14], many scholars have carried out model experiments on the stiffness of segment joints [15–21].

However, according to the beam-spring model, it is difficult to obtain the analytical solution of the segment ring under the external load, and it is not convenient to quantify the influence of the joint stiffness on the internal force. The mechanical study of the segment should follow the philosophy of the component prior to the structure. As a concrete component, although the mechanical properties of the segment can be improved by adding admixture and other means [22–24], the analysis of the model of segment component based on discontinuous joints should be paid more attention. The mechanical feature of the segment component is that a certain amount of deformation is allowed at the joint. An in-depth analysis of this feature will help to better serve the segment design.

Although there have been extensive studies on the buckling stability of arched components [25–29], few studies have explored the analytical solution of the internal force of the segment with the influence of joints. To be close to reality, a spring was used in the model studied in this paper to simulate the effect of the joint on the segment component. Under an external load, displacements occur at the joints, causing the internal force of the joints to change, which in turn affects the internal force distribution of the segment component. Therefore, it is crucial to study the influence of the displacements or stiffness of the segment joints on the internal force of the segment. The objective of this paper is to investigate the mechanical properties of a segment component with a discontinuous joint, including joint rotation

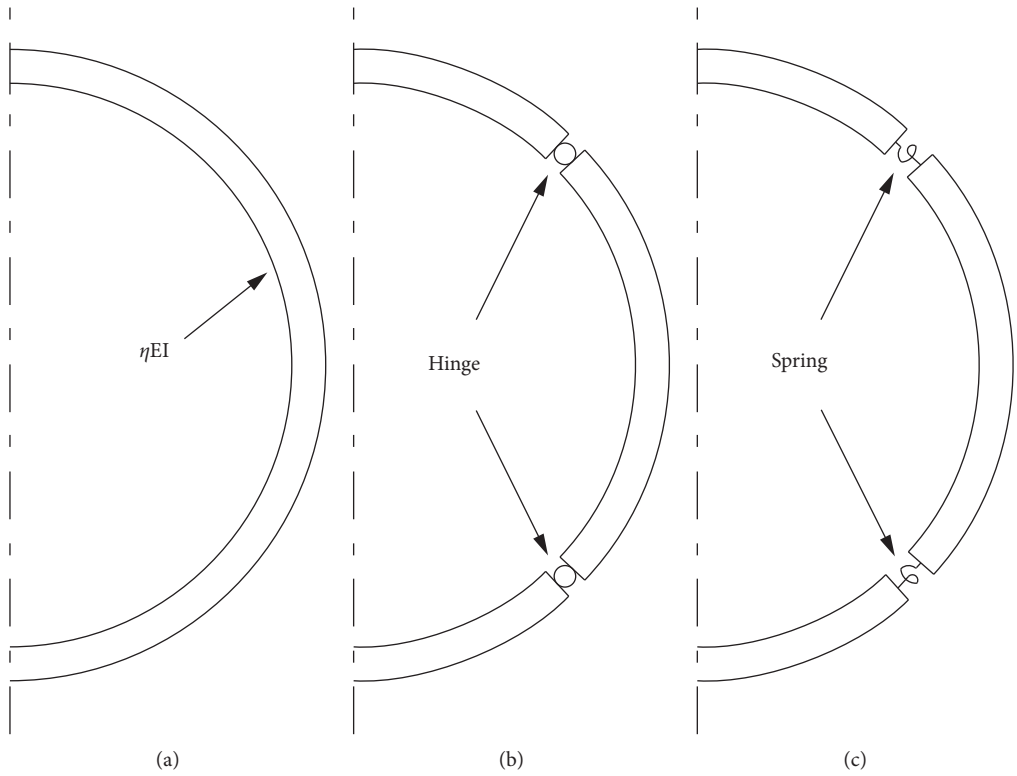

Figure 1: Calculation models of the segment ring: (a) uniform rigid ring, (b) multihinge ring, and (c) beam-spring model.

and translation. Based on the mechanical properties of the segment component, we propose a progressive model to analyse the internal force of the segment component under joint rotation and translation. Using the elastic centre method and the superposition principle, the internal force calculation formula for a segment component with discontinuous joints is deduced. The theoretical analysis is used to study the internal forces of a fabricated subway subsurface excavation section from the starting point to Jin'anqiao on Beijing Metro Line 6. Based on the load test data of the segment joints, spline interpolation and iterative method are used to solve the internal force of the segment component under the action of earth pressure. The theoretical analysis and the calculation results in this study provide a reference for future segment design.

2. Mechanical Model of the Segment Component

2.1. Basic Assumptions and the Model Establishment. Compared with the joint stiffness, the stiffness of the segment is greater, and thus, the joints will have a larger rotation or translation under the action of the external load compared to the segment. The segment component is a statically indeterminate structure with a redundant constraint, and therefore, the displacements of the joints inevitably have an effect on the distribution of the internal force of the segment.

To simplify the calculation, the internal force distribution of a single segment component under uniform pressure in the direction of the vertical span is studied. To evaluate the effect of the discontinuous rotation and translation between the joints and the segment, the segment component is considered to consist of a single segment and the joints on both sides that constrain the displacement of the segment. The constraint at the segment joints is simplified to consist of a rotational spring and two orthogonal line springs. The rotational spring constrains the rotation of the segment component and allows rotational displacement to occur under an external load. The linear spring constrains the movement of the segment component and allows for linear displacement under an external load. In order to make the analytical model consistent with the boundary conditions of the segment joint load test and to simplify the calculation, this analysis model does not consider the interaction between the segment and the soil. The mechanical model of the segment component is shown in Figure 2.

α is the semiarc angle of the segment component, l is the span length of the segment, R is the radius of the segment component, q is the uniform pressure perpendicular to the span, θ is the angular displacements of the segment joints, Δ_1 is the horizontal displacement of the segment joints, and Δ_2 is the vertical displacement of the segment joints.

In addition, it should be noted that in the calculation of internal force, a positive sign is assigned to the bending moment when the inside of the segment component is subjected to tension, a positive sign is assigned to the shear force when the moment of the adjacent section caused by the shear force is clockwise, and a positive sign is assigned to the axial force when the section is compressed.

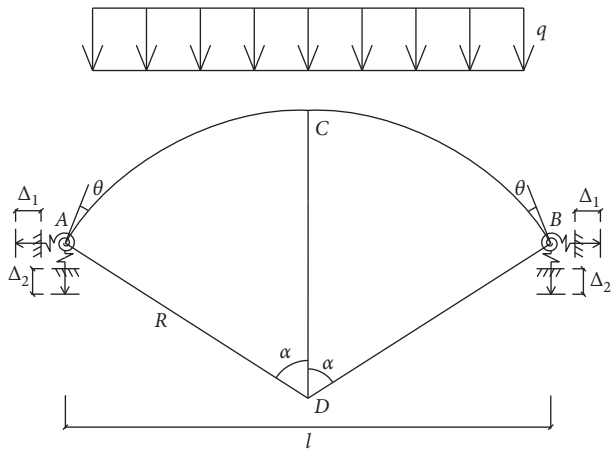

Figure 2: Force diagram of the segment component.

2.2. Model Simplification. According to the principle of superposition, the stress state of the segment component under an external load is decomposed into two parts when solving the internal force distribution. One is the internal force of the segment component under the external load when the segment joints are treated as the fixed ends. The other is the internal force of the segment component caused by the segment joints displacement.

The segment component is a statically indeterminate structure that can be solved by the force method equation. To simplify the calculation, the elastic centre method for the arched structure can be used to obtain the redundant force at the elastic centre. Then, we can obtain the internal force distribution of the segment component. The calculation diagrams in the two states are shown in Figures 3 and 4.

M_c, V_c, and N_c are the redundant bending moment, redundant shear force, and redundant axial force at the elastic centre of the segment component under an external load or the load produced by the joint displacements, d is the vertical distance between the elastic centre point and the segment joints, and l is the span length of the segment component.

3. Internal Force Calculation of the Segment Component

3.1. Redundant Force Analysis of the Segment Component. The vertical distance between the elastic centre point O' and the segment joints can be obtained as follows:

$$d = \frac{\int (y'/\mathrm{EI})\mathrm{d}s}{\int (1/\mathrm{EI})\mathrm{d}s} = \left(\frac{1}{2\alpha} - \frac{1-4\rho^2}{8\rho}\right)l, \tag{1}$$

where α is the semiarc angle of the segment component and ρ is the rise-span ratio of the segment.

Under an external load without considering the joint displacements, using the elastic centre method, the redundant force at the elastic centre of the segment component can be deduced as follows:

$$\begin{cases} M_C = B_1 q l^2, \\ H_C = C_1 \dfrac{q l^2}{f}, \\ V_C = 0, \end{cases} \tag{2}$$

where f is the vector height of the segment and B_1 and C_1 are related to the rise-span ratio and the semiarc angle of the segment, which can be defined by the following expression:

$$\begin{aligned} B_1 &= \frac{1}{256\rho^2}\left[\left(1+4\rho^2\right)^2 - \frac{4\rho}{\alpha}\left(1-4\rho^2\right)\right], \\ C_1 &= \frac{\rho}{12\Phi}\left[\alpha\left(3-8\rho^2+48\rho^4\right) - 12\rho\left(1-4\rho^2\right)\right], \end{aligned} \tag{3}$$

where Φ is the affiliated coefficient, which can be defined by the following expression:

$$\Phi = \left(1+4\rho^2\right)^2\alpha^2 + 4\rho\left(1-4\rho^2\right)\alpha - 32\rho^2. \tag{4}$$

The redundant force at the elastic centre can affect the internal force distribution of the segment component. Equation (2) illustrates that under uniform pressure perpendicular to the span, the internal force of the segment component is related to the semiarc angle and the span length.

Under the load produced by the joint displacements, using the elastic centre method, the redundant force at the

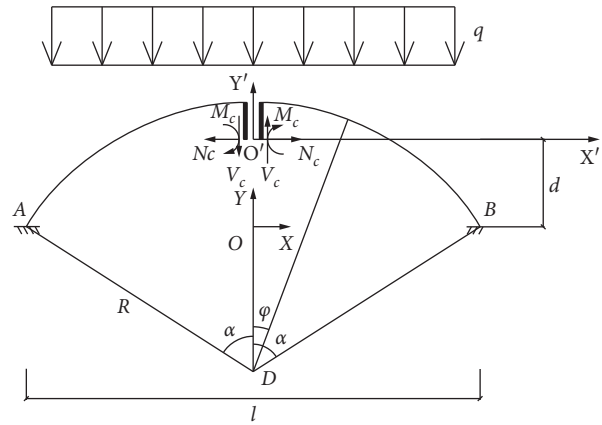

Figure 3: Force diagram of the segment component under an external load without considering the joint displacements.

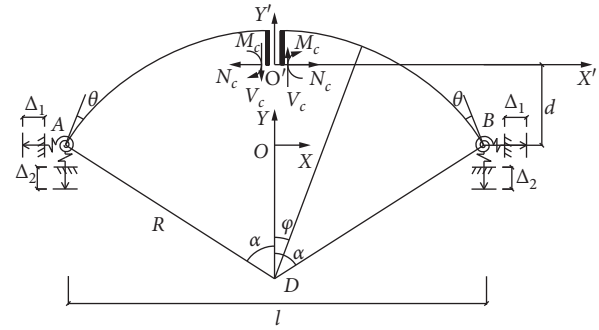

Figure 4: Force diagram of the segment component under the load produced by the joint displacements.

elastic centre of the segment component can be deduced as follows:

$$\begin{cases} M_C = -\dfrac{8\rho}{1-16\rho^4}\dfrac{\mathrm{EI}\theta}{l}, \\ H_C = -\dfrac{32\rho^2\left[16\rho^2 - 4\alpha\rho\left(1-4\rho^2\right)\right]}{\left(1+4\rho^2\right)\Phi}\dfrac{\mathrm{EI}\theta}{fl} - \dfrac{1024\rho^5\alpha}{\left(1+4\rho^2\right)\Phi}\dfrac{\mathrm{EI}\Delta_1}{f^2 l}, \\ V_C = 0, \end{cases} \tag{5}$$

where EI is the bending stiffness of the segment cross section.

Equation (5) can be analysed to obtain the following conclusions:

(1) If the vertical displacements on both sides of the segment component are consistent, the internal force of the segment will not be affected

(2) The internal force of the segment component produced by the joint displacements is affected not only by the radius and semiarc angle of the component but also by the joint rotation, the joint horizontal dislocation, and the bending stiffness of the segment

3.2. Internal Force Calculation of the Segment Component. From the redundant force at the elastic centre, we can obtain the internal force of the segment component under an external load with considering the joint displacements:

$$\begin{cases} M_\varphi = -\dfrac{1}{2}qR^2\sin^2\varphi + \left(B_1ql^2 - \dfrac{8\rho}{1-16\rho^4}\dfrac{\mathrm{EI}\theta}{l}\right) + \left(C_1\dfrac{ql^2}{f} - \dfrac{128\rho^3\left[4\rho-\alpha\left(1-4\rho^2\right)\right]}{\left(1+4\rho^2\right)\Phi}\dfrac{\mathrm{EI}\theta}{fl} - \dfrac{1024\rho^5\alpha}{\left(1+4\rho^2\right)\Phi}\dfrac{\mathrm{EI}\Delta_1}{f^2l}\right) \\ \qquad \cdot(d + R\cos\alpha - R\cos\varphi), \\ V_\varphi = -qR\sin\varphi\cos\varphi + \left(C_1\dfrac{ql^2}{f} - \dfrac{128\rho^3\left[4\rho-\alpha\left(1-4\rho^2\right)\right]}{\left(1+4\rho^2\right)\Phi}\dfrac{\mathrm{EI}\theta}{fl} - \dfrac{1024\rho^5\alpha}{\left(1+4\rho^2\right)\Phi}\dfrac{\mathrm{EI}\Delta_1}{f^2l}\right)\sin\varphi, \\ N_\varphi = qR\sin^2\varphi + \left(C_1\dfrac{ql^2}{f} - \dfrac{128\rho^3\left[4\rho-\alpha\left(1-4\rho^2\right)\right]}{\left(1+4\rho^2\right)\Phi}\dfrac{\mathrm{EI}\theta}{fl} - \dfrac{1024\rho^5\alpha}{\left(1+4\rho^2\right)\Phi}\dfrac{\mathrm{EI}\Delta_1}{f^2l}\right)\cos\varphi, \end{cases} \tag{6}$$

where φ is arc angles of the sectional segment.

Equation (6) reveals that the internal force of the segment component is affected by the joint rotation and horizontal dislocation when the segment section and the block mode are fixed.

Before the internal force calculation of the segment components, the final joint deformation cannot be predicted. However, the rotation and horizontal displacement of the segment joints can be calculated by the joint bending stiffness and shear stiffness, respectively.

It is assumed that the bending stiffness of the segment joints is k_θ. We can determine that

$$\theta = \frac{M_\alpha}{k_\theta}, \tag{7}$$

where M_α is the section bending moment of the segment component, when the semiarc angle is α. After substituting equation (6) into equation (7), the following equation is obtained:

$$\theta = \frac{B_1ql^2 + \left(C_1\left(ql^2/f\right) - \left(1024\rho^5\alpha/\left(1+4\rho^2\right)\Phi\right)\left(\mathrm{EI}\Delta_1/f^2l\right)\right)d - (1/2)qR^2\sin^2\alpha}{k_\theta + \left(8\rho/\left(1-16\rho^4\right)\right)(\mathrm{EI}/l) + \left(128\rho^2\left[4\rho^2 - \alpha\rho\left(1-4\rho^2\right)\right]/\left(\left(1+4\rho^2\right)\Phi\right)\right)(\mathrm{EI}/fl)d}, \tag{8}$$

where k_θ is the bending stiffness of the segment joints.

After substituting equations (8) and $\sin\alpha = (4\rho/(1+4\rho^2))$ into equation (6), we can obtain the internal force of each segment section under the influence of the joints. The formula is more complex and is not shown here.

The stiffness of the joints is weakened, which causes the redistribution of the internal force of the segment component. We should consider the influence of the joint bending stiffness on the segment component when the segment section and the block mode are fixed.

The calculation method for the influence of the shear stiffness and bending stiffness of the discontinuous joint on the internal force of the segment component is similar and therefore not repeated.

4. Practical Engineering Application

4.1. Engineering Background. Our study takes a segment of the subsurface excavation section from the starting point to Jin'anqiao station of Beijing Metro Line 6 as the research object. The influence of discontinuous joints on the mechanical properties of the segment component is studied quantitatively. The assembly form of the subsurface excavation tunnel lining is used as a reference for that of the shield. However, there are obvious differences between this construction method and the shield method. After using the mining method to excavate the tunnel section and taking the initial support measure, the assembly of the segment depends on a special assembly machine. The segment section is shown in Figure 5. This method can overcome the disadvantages of shield tunnelling used in some special composite strata, such as quaternary stratum with upper soft and lower hard characteristics, rock stratum, composite stratum of rock and soil, and stratum containing spherical weathering bodies. The construction method combines the advantages of the mining method and shield method, is adaptable, and has a high degree of automation. It can also increase construction speed and enhance safety. In addition, the horseshoe tunnel increases the utilization of the excavation section.

4.2. Geological Condition. The lithological log mostly consists of plain fill, clayey silt, silty clay, gravel, and mixed gravel and silty clay from the top to bottom around the tunnel. The geological profile of the fabricated section is shown in Figure 6.

4.3. Theoretical Calculation and Analysis. The load can be calculated according to the calculation method of the tunnel with the mining method. To simplify the calculation, the vertical earth pressure is regarded as the load in the direction of the vertical span. The calculated vertical earth pressure is $q = 256.88$ kPa. Taking the geometrical parameters of the

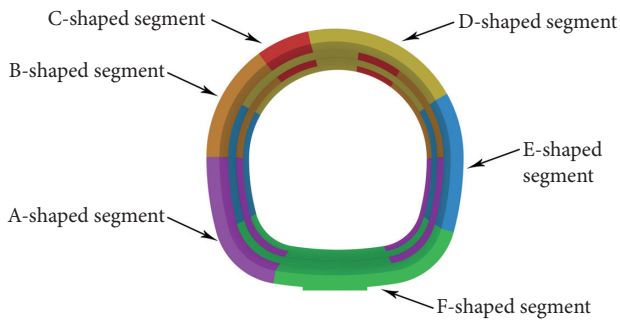

Figure 5: Segment section form.

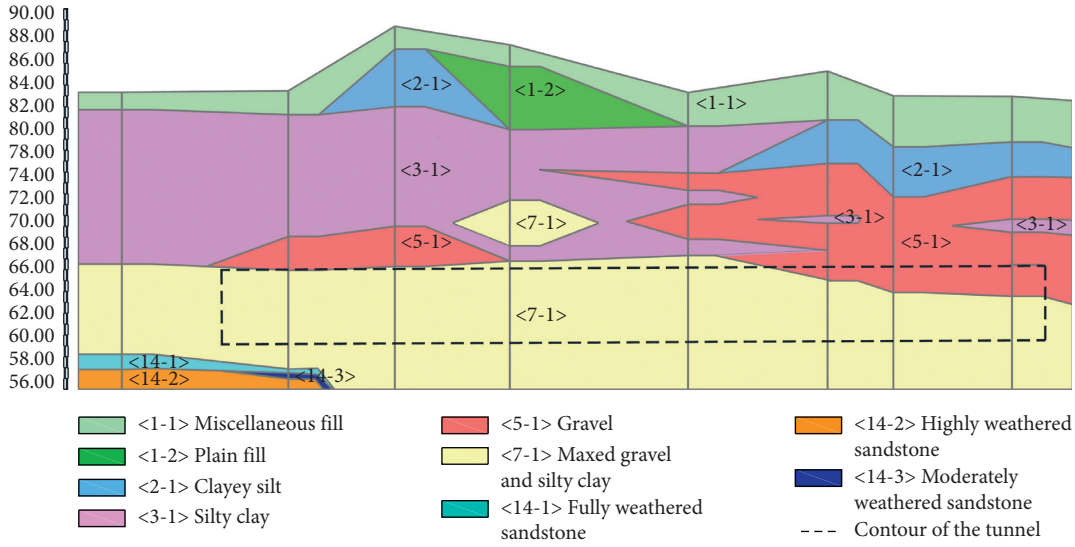

Figure 6: Geological sectional drawing of the fabricated section.

D-shaped segment, with a radius of 2.84 m, a thickness of 0.3 m, and a semiarc angle of 0.4π, as an example, the influence of joint deformation and stiffness on the internal force of the segment component was studied under the vertical load. Because the segment component and the external load are symmetrical along the vertical axes, only the internal force of the right half of the segment component is analysed.

Compiling the program through the M language in MATLAB, we can obtain the segment internal force distribution for joint angular displacements of 0.0000, 0.0002, or 0.0004 rad, as shown in Figure 7. The segment internal force distribution for joint horizontal displacements of 0, 2, or 4 mm is shown in Figure 8.

Figures 7 and 8 show that, under alignment, the maximum bending moment of the segment is 0.11 kN·m and the minimum bending moment is −0.05 kN·m. The maximum shear force is 270.63 kN, and the minimum shear force is −63.64 kN. The maximum axial force is 817.62 kN, and the minimum axial force is 510.00 kN. When the joint rotation angle is 0.0004 rad, the maximum bending moment of the segment is 0.05 kN·m and the minimum bending moment is −0.08 kN·m. The maximum shear force is 241.08 kN, and the minimum shear force is −77.26 kN. The maximum axial force is 807.87 kN, and the minimum axial force is 478.93 kN. When the joint horizontal displacement is 4 mm, the maximum bending moment of the segment is 0.21 kN·m and the minimum bending moment is −0.20 kN·m. The maximum shear force is 38.27 kN, and the minimum shear force is −190.11 kN. The maximum axial force is 741.97 kN, and the minimum axial force is 266.68 kN.

Figures 7 and 8 indicate that joint displacements can affect the internal force distribution of the segment component. The following observations can be made from the two figures:

(1) The joint rotation decreases the joint shear force while reducing the bending moment of the joints. The horizontal dislocation of the joints has a great effect on the bending moment of the segment component while reducing the shear force of the segment joints, and thus, the bending moment distribution is even more uneven. The axial force of the segment component is decreased due to the joint rotation and horizontal dislocation.

(2) The joint displacements cause a similar unloading effect on the internal force of the segment joints. The bending moment and shear force at other cross

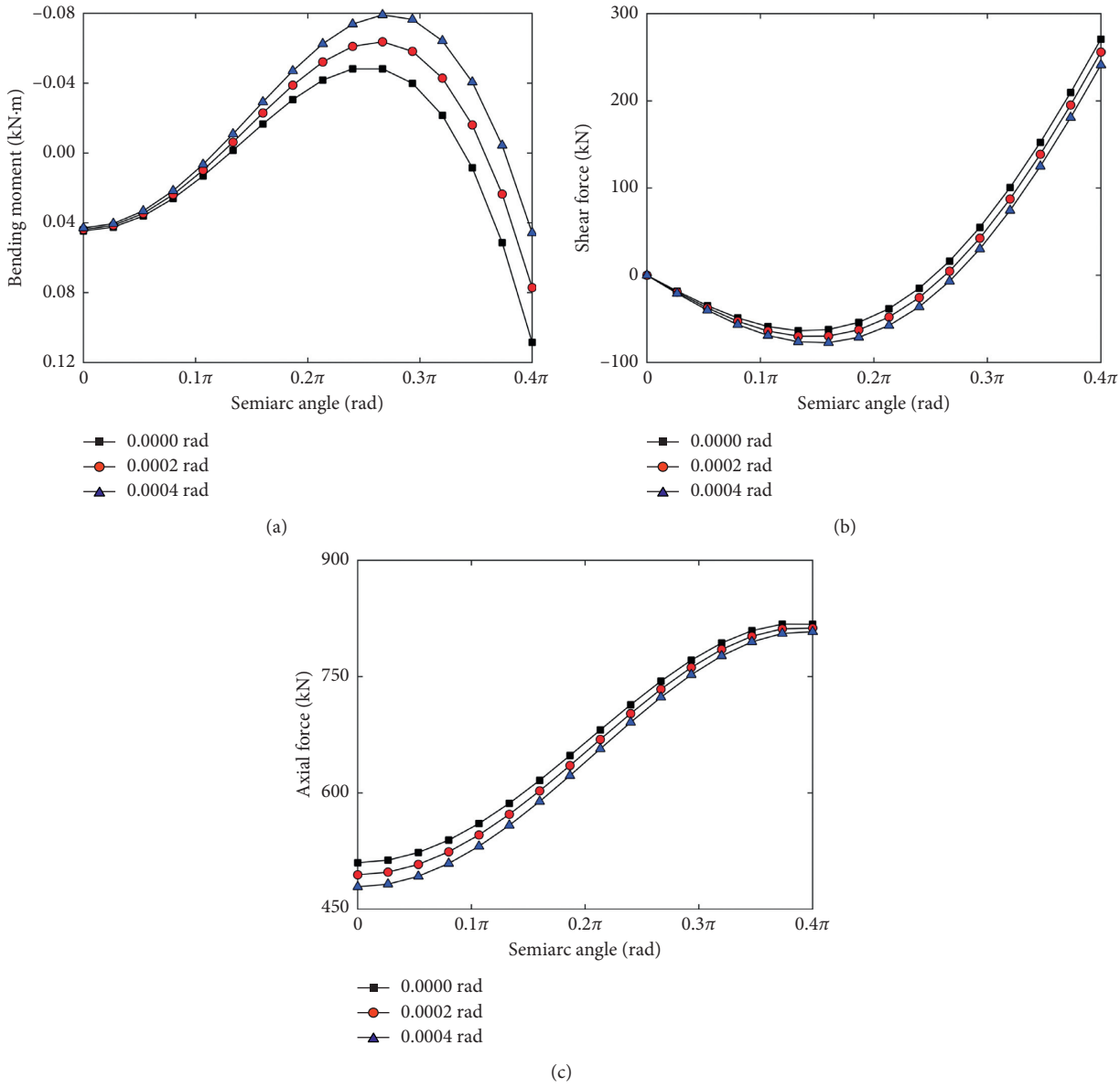

Figure 7: Internal force distribution of the segment component with joint rotation.

sections of the segment component will increase to different degrees, and the axial force of the segment component can be reduced, which should be considered in the structure calculation.

(3) The horizontal dislocation of the segment joints has a great influence on the internal force of the segment component.

In addition, relevant research data [30] and specification data [31] show that the control value of the horizontal dislocation is 10 mm. Under a maximum joint misalignment of 10 mm, the maximum bending moment of the segment is 0.47 kN·m and the minimum bending moment is −0.67 kN·m. The maximum shear force is 0 kN, and the minimum shear force is −437.69 kN. The maximum axial force is 628.72 kN, and the minimum axial force is −100.81 kN. By comparing with the internal force of the segment component with alignment, it can be obtained that the displacement of the segment has a great influence on the internal force distribution of the segment component. The bending moment varies the most, followed by the shear force.

The segment internal force distributions with joint bending rigidities of EI, 0.1EI, and 0.01EI are shown in Figure 9.

Analysis of Figure 9 reveals the following:

(1) As the joint bending stiffness decreases, the bending moment of the joints is decreased, and the internal force of the segment component is redistributed

(2) When the bending stiffness of the joints is equal to 0.01 times that of the segment, the bending moment of the segment joints is smaller and can be regarded as a hinge

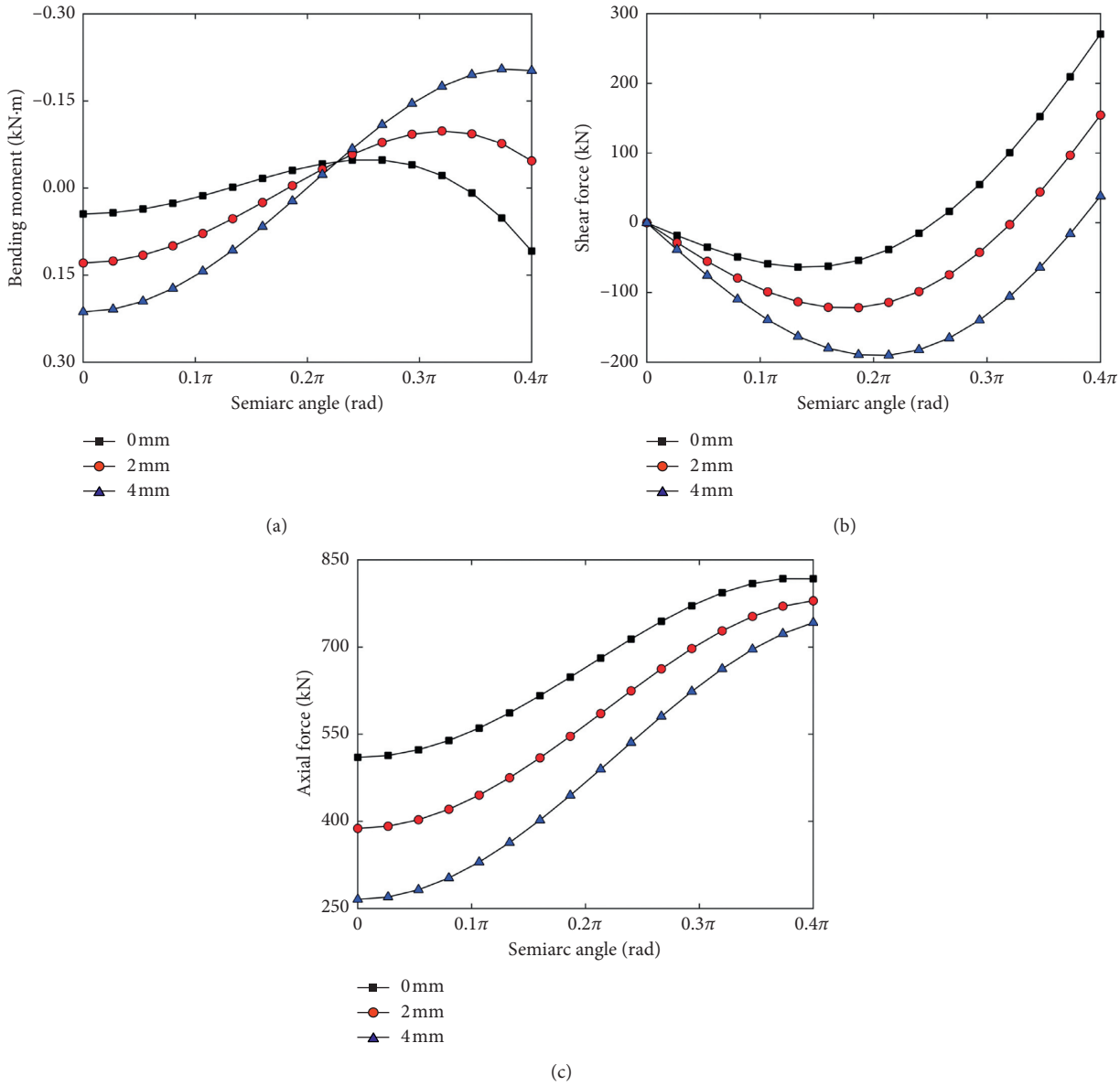

Figure 8: Internal force distribution of the segment component with joint horizontal dislocation.

(3) The effect of the bending stiffness of the discontinuous joint on the internal force of the segment actually reflects the influence of the joint rotation on this force

4.4. Test and Iterative Calculation. The bending stiffness of the segment joint is the bending moment required for the segment joint to produce a unit rotational angle. At present, there is no mature formula or chart available for the value of bending stiffness in the project, which can be determined by the segment joint load test [32].

In the test, the horizontal axial force is applied by the loading system on the reaction wall, and the vertical load is applied by the jack through the distribution beam. The test diagram is shown in Figure 10. According to the research results of the segment joint load test in Figure 11 [33], the joint stiffness of the segment is not constant. The larger the eccentric distance at the segment joints, the smaller the bending stiffness of the joints. When the eccentricity is constant, the greater the axial force at the segment joints, the smaller the bending stiffness of the joints.

From the above analysis, the eccentricity and axial force at the joint have an influence on the bending stiffness of the segment joints. The change of the bending stiffness at the joint inevitably causes the change of the joint displacement, which in turn causes the change of the internal force of the segment joints. The bending stiffness at the joint interacts with the internal force at the joint.

When analysing the mechanical model, the ultimate internal force at the joint cannot be predicted, so the bending stiffness of the joint cannot be selected from the data of the joint load test. Therefore, the iterative method is used to

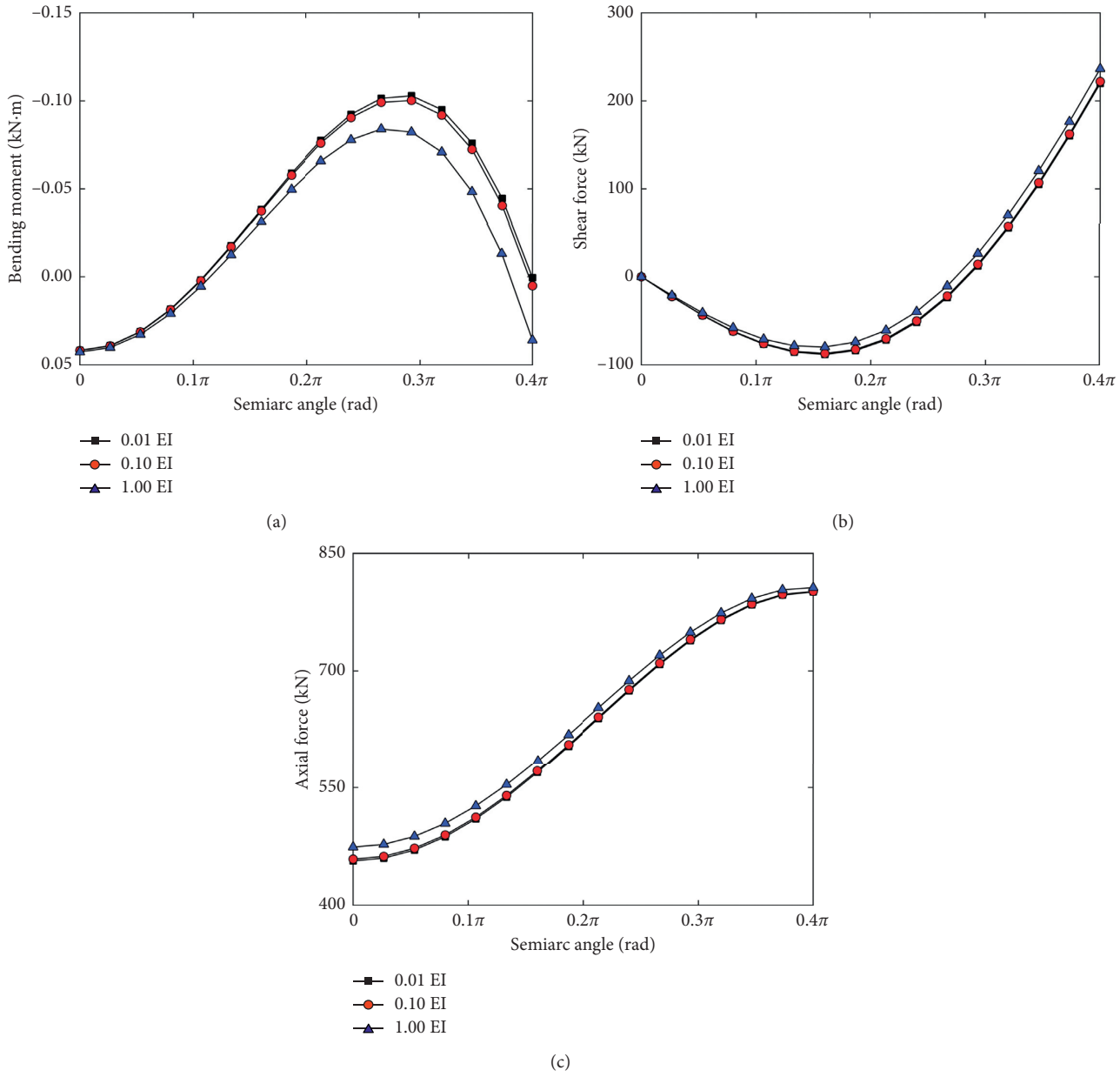

Figure 9: Internal force distribution of the segment component with joint bending stiffness changes.

repeatedly calculate the internal force of the segment and the joint stiffness and then successively approximate the true value to obtain the final internal force value.

In order to ensure the good convergence and continuity of the interpolation points, when selecting the bending stiffness of the joints, the data obtained from the load test of the segment joints should be calculated by spline interpolation. Algorithms of spline interpolation can be expressed as follows:

$$S(x) = \sum_{j=0}^{n} \left[y_j \alpha_j(x) + m_j \beta_j(x) \right], \tag{9}$$

where $S(x)$ is the interpolation function, y_j is the function value of node x_j, m_j is the derivative value of interpolation function, and $\alpha_j(x)$ and $\beta_j(x)$ are the interpolation basis functions.

The internal force of the segment and the stiffness of the segment joint are calculated by an iterative method. By compiling the program, we can get the internal force distribution of the segment component, which is shown in Figure 12.

After iterative calculation, the final bending stiffness of the segment joint is 1.2×10^4 kN·m·rad^{-1}.

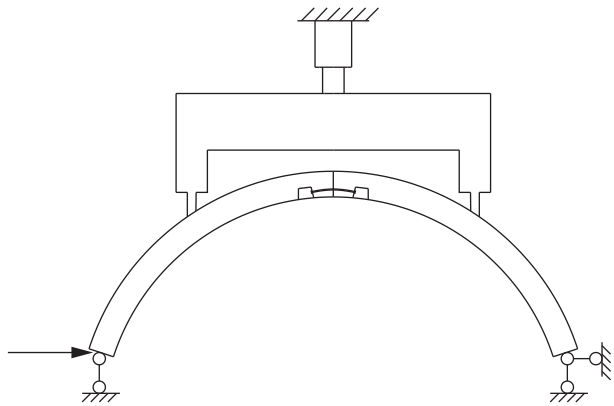

Figure 10: Diagram of the joint load test of the segment.

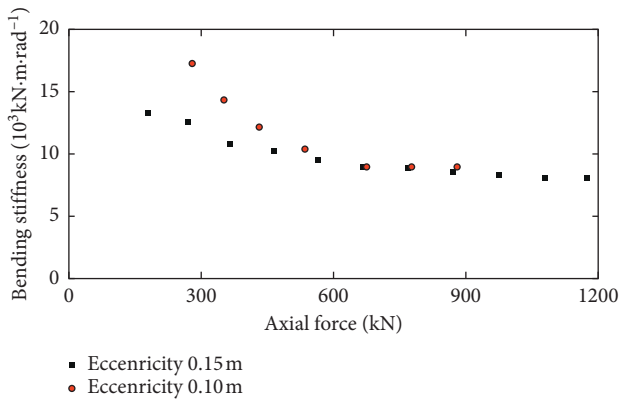

Figure 11: Joint load test data.

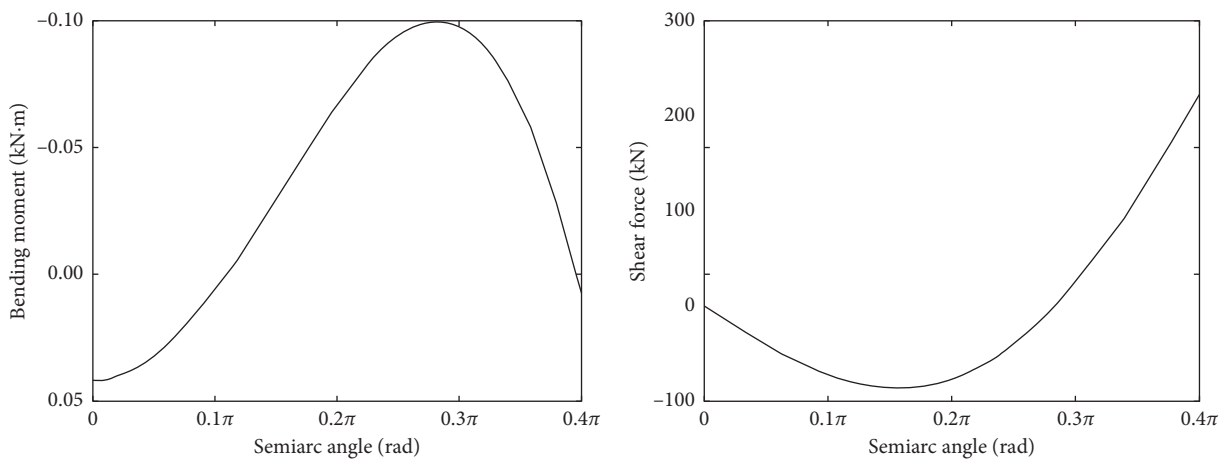

Figure 12: Continued.

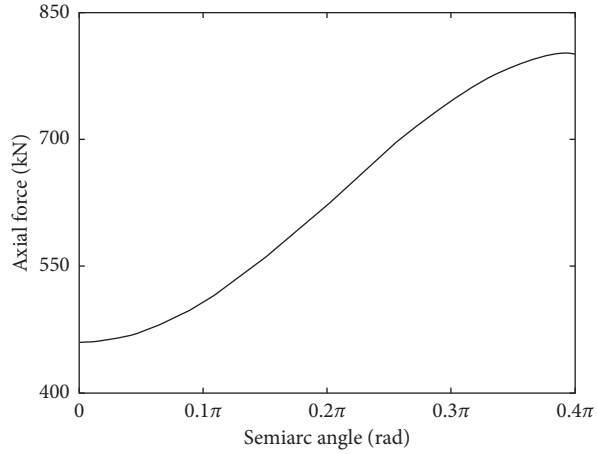

Figure 12: Internal force of the segment component calculated by iteration.

5. Conclusions

In view of the lack of analytical research on the internal force of the segment component, based on the mechanical characteristics of the segment component, that is, a certain amount of deformation is allowed at the segment joints, the internal force of the segment component is analysed deeply. The mechanical model of the segment component under the elastic constraint is established, and the analytic solution of the internal force of the segment component with discontinuous joints is solved by using the elastic centre method and the superposition principle. Combined with the engineering application, the following conclusions can be drawn based on the above analysis:

(1) The internal force of the segment component with discontinuous joints is affected by the radius, the semiarc angle, the joint rotation, the horizontal dislocation, the segment bending stiffness, the joint bending stiffness, and other factors.

(2) The joint rotation reduces the bending moment, the shear force, and the axial force of the segment joints, and the joint horizontal dislocation reduces the shear force and axial force of the segment joints. The joint displacements increase the negative bending moment and the negative shear force of the segment component to different degrees. The adverse effect should be considered in the segment design by taking measures such as increasing the reinforcement ratio of the segment section and reducing the joint displacements.

(3) The joint horizontal dislocation has a greater effect on the internal force of the segment component than does the joint rotation. In the control of joint displacements, we should pay attention to restraining the dislocation displacements.

(4) As the bending stiffness decreases, the negative bending moment of the segment component increases, and the nonuniformity of the segment bending moment is increased.

(5) To maintain a uniform internal force of the segment component, when the segment is designed, joints such as the tenon joint should be strengthened to reduce the internal force of the segment section, in addition to applying other relevant methods.

(6) Since the bending stiffness of the joints is related to the internal force of that, the internal force of the segment component and the joint stiffness should be iteratively calculated in combination with the research results of the joint load test.

(7) Studies of the analytical solution of the internal force of the segment component with discontinuous joints can aid the identification of factors that affect the internal force of the segment, which can be used as the basis for the analytical calculation of the whole segment ring with discontinuous joints.

Data Availability

The data that support the findings of this study are available within the article.

Conflicts of Interest

The authors declare that they have no conflicts of interest.

Authors' Contributions

Linwei Dong conceptualized the study and was responsible for methodology; Linwei Dong and Zhiyong Yang performed formal analysis; Linwei Dong and Zhenyong Wang prepared the original draft; Linwei Dong, Zhiyong Yang, Zhenyong Wang, Yaowen Ding, and Weiqiang Qi reviewed and edited the manuscript; Zhiyong Yang was involved in study supervision and funding acquisition.

Acknowledgments

This work was supported by the National Natural Science Foundation of China (Grant no. U1261212) and Beijing Municipal Education Commission (Grant no. ZDZH20141141301).

References

[1] G. Y. Cui, X. L. Wang, Z. Z. Wang, and D. Y. Wang, "Model tests on the antibreaking countermeasures for tunnel lining across stick-slip faults," *Advances in Materials Science and Engineering*, vol. 2020, Article ID 7937595, 10 pages, 2020.

[2] J. R. Standing and C. Lau, "Small-scale model for investigating tunnel lining deformations," *Tunnelling and Underground Space Technology*, vol. 68, pp. 130–141, 2017.

[3] C. Shi, C. Cao, M. Lei, L. Peng, and H. Ai, "Effects of lateral unloading on the mechanical and deformation performance of shield tunnel segment joints," *Tunnelling and Underground Space Technology*, vol. 51, pp. 175–188, 2016.

[4] C. B. M. Blom, *Design philosophy of concrete linings for tunnels in soft soils*, Ph.D. thesis, Delft University of Technology, Delft, The Netherlands, 2004.

[5] R. B. Peck, A. J. Hendron, and B. Mohraz, "State of the art of soft-ground tunneling," in *Proceedings of the 1st Rapid Excavation and Tunnel Conference*, pp. 259–286, Chicago, IL, USA, June 1972.

[6] A. M. M. Wood, "The circular tunnel in elastic ground," *Géotechnique*, vol. 25, no. 1, pp. 115–127, 1975.

[7] D. J. Yang and X. Wang, "Study on flexural rigidity of segment joints in metro shield tunnel," *Applied Mechanics and Materials*, vol. 170–173, pp. 1716–1721, 2012.

[8] X. Zhong, W. Zhu, Z. Huang, and Y. Han, "Effect of joint structure on joint stiffness for shield tunnel lining," *Tunnelling and Underground Space Technology*, vol. 21, pp. 406-407, 2016.

[9] Y. Koyama, "Present status and technology of shield tunneling method in Japan," *Tunnelling and Underground Space Technology*, vol. 18, no. 2-3, pp. 145–159, 2003.

[10] International Tunnelling Association, "Guidelines for the design of shield tunnel lining," *Tunnelling and Underground Space Technology*, vol. 15, no. 3, pp. 303–331, 2000.

[11] H. Zhao, X. Liu, Y. Bao, and Y. Yuan, "Nonlinear simulation of tunnel linings with a simplified numerical modelling," *Structural Engineering and Mechanics*, vol. 61, no. 5, pp. 593–603, 2017.

[12] X. Liu, Y. Zhang, and Y. Bao, "Full-scale experimental investigation on stagger effect of segmental tunnel linings," *Tunnelling and Underground Space Technology*, vol. 102, Article ID 103423, 2020.

[13] F. Yang, S. Cao, and Q. Li, "An analytical model for the rotational behavior of concrete segmental joints with gaskets," *Advances in Structural Engineering*, vol. 22, no. 13, pp. 2866–2881, 2019.

[14] C. He, S. Zhou, P. Guo, H. Di, and X. Zhang, "A theoretical model on the influence of ring joint stiffness on dynamic responses from underground tunnels," *Construction and Building Materials*, vol. 223, pp. 69–80, 2019.

[15] A. Caratelli, A. Meda, Z. Rinaldi, S. Giuliani-Leonardi, and F. Renault, "On the behavior of radial joints in segmental tunnel linings," *Tunnelling and Underground Space Technology*, vol. 71, pp. 180–192, 2018.

[16] X. Liu, Z. Dong, W. Song, and Y. Bai, "Investigation of the structural effect induced by stagger joints in segmental tunnel linings: direct insight from mechanical behaviors of longitudinal and circumferential joints," *Tunnelling and Underground Space Technology*, vol. 71, pp. 271–291, 2018.

[17] A. Tsiampousi, J. Yu, J. Standing, R. Vollum, and D. Potts, "Behaviour of bolted cast iron joints," *Tunnelling and Underground Space Technology*, vol. 68, pp. 113–129, 2017.

[18] L. Zuo, G. Li, K. Feng et al., "Experimental analysis of mechanical behavior of segmental joint for gas pipeline shield tunnel under unfavorable compression-bending loads," *Tunnelling and Underground Space Technology*, vol. 77, pp. 227–236, 2018.

[19] K. Feng, C. He, Y. Qiu et al., "Full-scale tests on bending behavior of segmental joints for large underwater shield tunnels," *Tunnelling and Underground Space Technology*, vol. 75, pp. 100–116, 2018.

[20] Q.-x. Yan, L.-y. Song, H. Chen, W.-y. Chen, S.-q. Ma, and W.-b. Yang, "Dynamic response of segment lining of overlapped shield tunnels under train-induced vibration loads," *Arabian Journal for Science and Engineering*, vol. 43, no. 10, pp. 5439–5455, 2018.

[21] Y. Jin, W. Ding, Z. Yan, K. Soga, and Z. Li, "Experimental investigation of the nonlinear behavior of segmental joints in a water-conveyance tunnel," *Tunnelling and Underground Space Technology*, vol. 68, pp. 153–166, 2017.

[22] L. Wang, F. Guo, H. Yang, Y. Wang, and S. Tang, "Comparison of fly ash, PVA fiber, Mgo and shrinkage-reducing admixture on the frost resistance of face slab concrete via pore structural and fractal analysis," *Fractals*, 2020.

[23] L. Wang, M. Jin, F. Guo, Y. Wang, and S. Tang, "Pore Structural and fractal analysis of the influence of fly ash and silica fume on the mechanical property and abrasion resistance of concrete," *Fractals*, 2020.

[24] L. Wang, R. Luo, W. Zhang, M. Jin, and S. Tang, "Effects of fineness and content of phosphorus slag on cement hydration, permeability, pore structure and fractal dimension of concrete," *Fractals*, 2020.

[25] X. Han, Y. Xia, X. Wang, and L. Chai, "Complex variable solutions for forces and displacements of circular lined tunnels," *Mathematical Problems in Engineering*, vol. 2018, Article ID 103423, 12 pages, 2018.

[26] N.-H. Lim and Y.-J. Kang, "Out of plane stability of circular arches," *International Journal of Mechanical Sciences*, vol. 46, no. 8, pp. 1115–1137, 2004.

[27] Y. S. Deng and Y. N. Wang, "Effects of skewback settlement on buckling performance of circular arch," *Engineering Journal of Wuhan University*, vol. 46, no. 6, pp. 772–775, 2013.

[28] C. Dou and Y. L. Guo, "Study on flexural-torsional buckling load of circular arches," *Engineering Mechanics*, vol. 29, no. 3, pp. 83–89, 2012.

[29] Y. L. Pi, M. A. Bradford, and Y. L. Guo, "Revisiting nonlinear in-plane elastic buckling and postbuckling analysis of shallow circular arches under a central concentrated load," *Journal of Engineering Mechanics*, vol. 142, no. 8, Article ID 04016046, 8 pages, 2016.

[30] Q. Zhang, S. J. Du, and M. J. Lu, "Research on dislocation monitoring for shield tunnel segments with straight joint," *Chinese Journal of Underground Space and Engineering*, vol. 4, no. 1, pp. 138–142, 2008.

[31] Ministry of Housing and Urban-Rural Development of the People's Republic of China, *GB 50446-2017 Code for Construction and Acceptance of Shield Tunnelling Method*, China Architecture and Building Press, Beijing, China, 2017.

[32] C. He and D. Y. Zeng, *The Structure Design of Shield Tunnel and the Impact of Construction on Environment*, Southwest Jiao Tong University Press, Chengdu, China, 2007.

[33] H. Y. Zhou, *Theoretical study and test on mechanic behavior of lining segment in shield tunnel dissertation*, Ph.D. thesis, Dalian University of Technology, Dalian, China, 2011.